

Effect of in-medium mass-shift on transverse-momentum spectrum and elliptic anisotropy of ϕ meson

Yong Zhang^{1,2*}, Jing Yang³, and Weihua Wu¹

¹*School of Mathematics and Physics, Jiangsu University of Technology, Changzhou, Jiangsu 213001, China*

²*School of Science, Inner Mongolia University of Science & Technology, Baotou, Inner Mongolia Autonomous Region 014010, China*

³*School of Physics and School of International Education Teachers, Changchun Normal University, Changchun, Jilin 130032, China*

(Dated: May 10, 2019)

We study the effect of in-medium mass-shift on transverse-momentum spectrum and elliptic anisotropy of ϕ meson. It is found that the mass-shift enhances the ϕ yields and suppresses the elliptic flow v_2 in large momentum region, and the effects increase with the increasing mass-shift. The effects are various for different sources and decrease with the increasing expanding velocity. We further study the effects for parts of all ϕ meson with mass-shift, and the effects decrease with the decreasing probability of ϕ meson with mass-shift. Since the different mass-shift lead to different transverse-momentum spectrum and v_2 , our study may provide a way to restrict the ranges of in-medium mass-shift of ϕ meson in high-energy heavy-ion collisions.

PACS numbers: 25.75.Dw, 25.75.Ld, 21.65.jk

I. INTRODUCTION

The main goal of high-energy heavy-ion collisions is to create the matter of quark-gluon plasma (QGP), and study its properties by analyzing the observables of particles in final state [1–4]. $\phi(s\bar{s})$ meson is an excellent probe for studying QGP because it is sensitive to several aspects of the collision [5–11] and it is expected to have a small interaction with the hadronic medium [5, 7, 8, 12–15]. However, the recent experimental data of the elliptic flow of identified hadrons in the Pb-Pb collisions at $\sqrt{s_{NN}} = 2.76$ GeV indicate that the ϕ meson may have a larger hadronic cross section than its current theoretical estimate [16]. It is still an open issue to determine the interaction between ϕ and the hadronic medium.

The transverse-momentum spectrum and elliptic flow of ϕ meson are important observables in high-energy heavy-ion collisions [6–11, 15, 16]. The transverse-momentum spectrum can reveal information about the thermalization and expansion of the ϕ emission source [6, 9–11], and the elliptic flow v_2 of ϕ meson was an important evidence for the formation of hot and dense matter with partonic collectivity [7, 8, 15, 16]. The ϕ meson is expected to have a mass-shift in the hadronic medium, and the mass-shift are various for several theoretical calculations [17–24]. In this work, we will study the effect of in-medium mass-shift on transverse-momentum spectrum and elliptic flow v_2 of ϕ meson, by using the ideal relativistic hydrodynamics in 2 + 1 dimensions to describe the transverse expansion of sources with zero net baryon density and combine the Bjorken boost-invariant hypothesis [25] for the source longitudinal evolution. In the calculations, we use the equation of state of s95p-

PCE [26] and take the initial energy density distribution in the transverse plane as the Gaussian distribution: $\epsilon = \epsilon_0 \exp[-x^2/(2R_x^2) - y^2/(2R_y^2)]$, where ϵ_0 and R_i ($i = x, y$) are the parameters of the initial source energy density and radii [27]. And the freeze-out temperature of ϕ is taken as 140 MeV [27–30].

This paper is organized as follows. In Sec. II, we present the formulas of the single-particle momentum distribution for boson with in-medium mass-shift. In Sec. III, the effect of mass-shift on the transverse momentum spectrum and the elliptic flow v_2 of ϕ meson will be shown. Finally, a summary of this paper are given in Sec. IV.

II. FORMULISM

Denote $a_{\mathbf{k}}$ ($a_{\mathbf{k}}^\dagger$) the annihilation (creation) operator of the free boson with momentum \mathbf{k} and mass m , and the invariant single-particle momentum distribution can be expressed by

$$N(\mathbf{k}) = \omega_{\mathbf{k}} \frac{d^3 N}{d\mathbf{k}} = \omega_{\mathbf{k}} \langle a_{\mathbf{k}}^\dagger a_{\mathbf{k}} \rangle, \quad (1)$$

where $\langle \dots \rangle$ means the thermal average, and $\omega_{\mathbf{k}} = \sqrt{\mathbf{k}^2 + m^2}$ is the energy of the free particle. For a homogeneous source with volume V and temperature T , the single particle momentum distribution becomes

$$N(\mathbf{k}) = \frac{V}{2\pi^3} \omega_{\mathbf{k}} n_B(\mathbf{k}), \quad (2)$$

$$n_B(\mathbf{k}) = \frac{1}{\exp(\omega_{\mathbf{k}}/T) - 1}. \quad (3)$$

Denote $b_{\mathbf{k}}$ ($b_{\mathbf{k}}^\dagger$) the annihilation (creation) operator of the boson with momentum \mathbf{k} and modified mass m_* ($m_* =$

*zhy913@jsut.edu.cn

$m - \delta m$) in hadronic medium. The operators ($a_{\mathbf{k}}, a_{\mathbf{k}}^\dagger$) and ($b_{\mathbf{k}}, b_{\mathbf{k}}^\dagger$) were related by the Bogoliubov transformation [28, 31]

$$a_{\mathbf{k}} = c_{\mathbf{k}} b_{\mathbf{k}} + s_{-\mathbf{k}}^* b_{-\mathbf{k}}^\dagger. \quad (4)$$

For a homogeneous source, $c_{\mathbf{k}} = \cosh f_{\mathbf{k}}$, $s_{\mathbf{k}} = \sinh f_{\mathbf{k}}$ and $f_{\mathbf{k}} = \frac{1}{2} \log(\omega_{\mathbf{k}}/\Omega_{\mathbf{k}})$. Where $\Omega_{\mathbf{k}} = \sqrt{\mathbf{k}^2 + m_*^2}$ is the energy of the particle in medium, and the single particle momentum distribution becomes [28, 29]

$$N(\mathbf{k}) = \frac{V}{2\pi^3} \omega_{\mathbf{k}} n_1(\mathbf{k}), \quad (5)$$

$$n_1(\mathbf{k}) = |c_{\mathbf{k}}|^2 n_{\mathbf{k}} + |s_{-\mathbf{k}}|^2 (n_{-\mathbf{k}} + 1), \quad (6)$$

$$n_{\mathbf{k}} = \frac{1}{\exp(\Omega_{\mathbf{k}}/T) - 1}, \quad (7)$$

as can be seen from equation (5) – (7), the single particle momentum distribution $N(\mathbf{k})$ changes with the particle mass in medium.

For hydrodynamic sources, the single particle momentum distribution of the boson without in-medium mass-shift was expressed as [32–34]

$$N_0(\mathbf{k}) = \int \frac{g_i}{(2\pi)^3} d^4\sigma_\mu(r) k^\mu n_{\mathbf{k}'}^0, \quad (8)$$

$$n_{\mathbf{k}'}^0 = \frac{1}{\exp(\omega_{\mathbf{k}'}(r)/T(r)) - 1}, \quad (9)$$

$$\omega_{\mathbf{k}'}(r) = \sqrt{\mathbf{k}'^2(r) + m^2} = k^\mu u_\mu(r), \quad (10)$$

and the single particle momentum distribution of the boson with in-medium mass-shift was expressed as [27–29, 35]

$$N_*(\mathbf{k}) = \int \frac{g_i}{(2\pi)^3} d^4\sigma_\mu(r) k^\mu \left\{ |c'_{\mathbf{k}'}|^2 n'_{\mathbf{k}'} + |s'_{-\mathbf{k}'}|^2 [n'_{-\mathbf{k}'} + 1] \right\}, \quad (11)$$

$$c'_{\pm\mathbf{k}'} = \cosh[f'_{\mathbf{k}'}], \quad s'_{\pm\mathbf{k}'} = \sinh[f'_{\mathbf{k}'}], \quad (12)$$

$$f'_{\mathbf{k}'} = \frac{1}{2} \log[\omega'_{\mathbf{k}'}/\Omega'_{\mathbf{k}'}] = \frac{1}{2} \log[k^\mu u_\mu(r)/k^{*\mu} u_\nu(r)], \quad (13)$$

$$\begin{aligned} \Omega'_{\mathbf{k}'}(r) &= \sqrt{\mathbf{k}'^2(r) + m_*^2} \\ &= \sqrt{[k^\mu u_\mu(r)]^2 - m^2 + m_*^2} \\ &= k^{*\mu} u_\mu(r), \end{aligned} \quad (14)$$

$$n'_{\pm\mathbf{k}'} = \frac{1}{\exp(\Omega_{\mathbf{k}'}(r)/T(r)) - 1}, \quad (15)$$

where g_i is the degeneracy factor for hadron species i . The quantity $d^4\sigma_\mu(r)$ is the four-dimension element of freeze-out hypersurface, and $u_\mu(r)$, $T(r)$ are the source four-velocity and temperature at freeze-out, respectively. $k^\mu = (\omega_{\mathbf{k}}, \mathbf{k})$ is the four-momentum of the particle, and \mathbf{k}' is the local-frame momentum corresponding to \mathbf{k} . If there is no mass-shift, the coefficients $|c'_{\mathbf{k}'}|^2$ and $|s'_{\mathbf{k}'}|^2$ will be 1 and 0, respectively. And $N_*(\mathbf{k})$ will be equal to $N_0(\mathbf{k})$.

III. RESULTS

In this section, we will present the results in three subsections. In section A, we will show the effect of in-medium mass-shift on the transverse momentum spectrum of ϕ . In section B, the effect of in-medium mass-shift on the elliptic flow v_2 will be shown. We further study the effect for parts of all ϕ mesons with mass-shift in section C.

A. Effect of in-medium mass-shift on the transverse momentum spectrum

In Fig. 1 (a) and (b), we show the normalized transverse momentum spectrum of ϕ meson with various mass-shift δm for the initial conditions $\epsilon_0 = 20$ and 40 GeV/fm³ and $R_x = 3$ fm, $R_y = 4$ fm. The ratio of the normalized transverse momentum spectrum with mass-shift to which without mass-shift is also shown in Fig. 1 (c) and (d). A small mass-shift leads to an increase in the yield of ϕ meson in large transverse momentum regions and thus reduce the slope of the transverse momentum spectrum, and the effect increases with the increasing mass-shift. For a fixed mass-shift, the transverse momentum spectrum for the initial conditions $\epsilon_0 = 20$ GeV/fm³ is more affected than for $\epsilon_0 = 40$ GeV/fm³.

With the Eq. (12) and (15), the Eq. (11) can be rewritten as

$$N_*(\mathbf{k}) = \int \frac{g_i}{(2\pi)^3} d^4\sigma_\mu(r) k^\mu [F_1 n'_{\mathbf{k}'} + F_2], \quad (16)$$

$$F_1 = 1 + 2F_2, \quad F_2 = |s'_{\mathbf{k}'}|^2, \quad (17)$$

the quantity $n'_{\mathbf{k}'}$ in Eq. (16) is approximately equal to the quantity $n_{\mathbf{k}'}^0$ in Eq. (8) for a small mass-shift, so the coefficient F_2 is the main factor for the particle spectrum.

In Fig. 2, we show the average coefficients $\overline{F_2}$ with various mass-shift and the ratio of $\overline{F_2}$ to $\overline{n'_{\mathbf{k}'}}$, where “—” means the average over all freeze-out points. The average coefficient $\overline{F_2}$ is very small (see Fig. 2 (a) and (b)) and the coefficient F_2 is positive, so the coefficient F_1 is approximately equal to 1 and the Eq. (16) can be rewritten as

$$N_*(\mathbf{k}) = \int \frac{g_i}{(2\pi)^3} d^4\sigma_\mu(r) k^\mu [n'_{\mathbf{k}'} + F_2]. \quad (18)$$

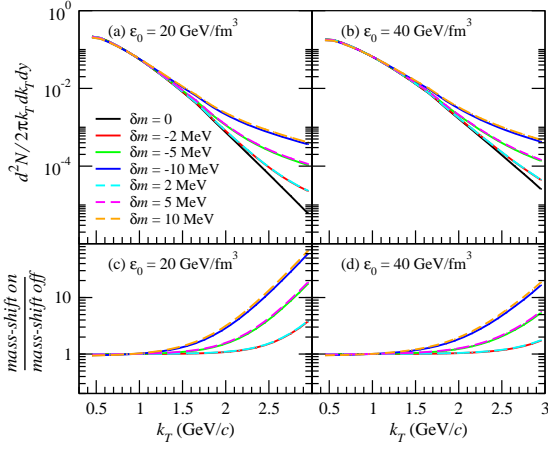


FIG. 1: (Color online) The normalized transverse momentum spectrum of ϕ meson with various mass-shift (top panel) and the ratio of the normalized transverse momentum spectrum with mass-shift to which without mass-shift (bottom panel) for the initial conditions $\epsilon_0 = 20$ and 40 GeV/fm³ and $R_x = 3$ fm, $R_y = 4$ fm.

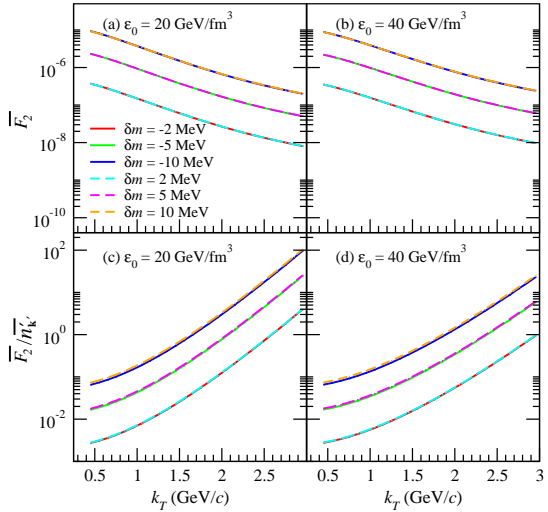


FIG. 2: (Color online) The average coefficient $\overline{F_2}$ with various mass-shift (top panel) and the ratio of $\overline{F_2}$ to $\overline{n'_k}$, where "—" means the average over all freeze-out points.

The ratio of $\overline{F_2}$ to $\overline{n'_k}$ increases with the increasing transverse momentum, so the effect of in-medium mass-shift on spectrum increases with the increasing transverse momentum (see Fig. 1). With the same mass-shift, the average coefficients $\overline{F_2}$ are almost the same for the initial conditions $\epsilon_0 = 20$ and 40 GeV/fm³. The high initial energy density leads to a large expanding velocity and thus increases the yield n'_k for large transverse momentum, so the ratio of $\overline{F_2}$ to $\overline{n'_k}$ for $\epsilon_0 = 40$ GeV/fm³ is smaller than for $\epsilon_0 = 20$ GeV/fm³ for a fixed mass-shift. This is the reason for the transverse momentum spectrum for $\epsilon_0 = 20$ GeV/fm³ is more affected than for $\epsilon_0 = 40$ GeV/fm³.

B. Effect of in-medium mass-shift on the elliptic flow

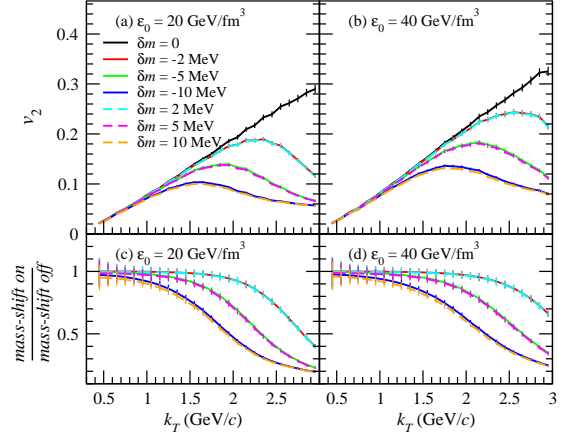


FIG. 3: (Color online) The v_2 of ϕ meson as a function of k_T with various mass-shift (top panel) and the ratio of v_2 of ϕ meson with mass-shift to which without mass-shift (bottom panel) for the initial conditions $\epsilon_0 = 20$ and 40 GeV/fm³ and $R_x = 3$ fm, $R_y = 4$ fm.

In Fig. 3, we show the v_2 of ϕ meson as a function of k_T with various mass-shift and the ratio of v_2 with mass-shift to which without mass-shift for the initial conditions $\epsilon_0 = 20$ and 40 GeV/fm³ and $R_x = 3$ fm, $R_y = 4$ fm. The v_2 of ϕ meson for $\epsilon_0 = 40$ GeV/fm³ is a little greater than for $\epsilon_0 = 20$ GeV/fm³ when there is no mass-shift ($\delta m = 0$). The v_2 is suppressed by a small mass-shift in large transverse momentum regions, and this effect increases with the increasing mass-shift. The suppression effect for $\epsilon_0 = 20$ GeV/fm³ is a little stronger than for $\epsilon_0 = 40$ GeV/fm³ (see Fig. 3 (c) and (d)).

To analyse the effect of mass-shift on v_2 , we rewrite the Eq. (18) as

$$\begin{aligned}
 N_*(\mathbf{k}) &= N_1(\mathbf{k}) + N_2(\mathbf{k}), \\
 N_1(\mathbf{k}) &= \int \frac{g_i}{(2\pi)^3} d^4\sigma_\mu(r) k^\mu n'_{\mathbf{k}'}, \\
 N_2(\mathbf{k}) &= \int \frac{g_i}{(2\pi)^3} d^4\sigma_\mu(r) k^\mu F_2.
 \end{aligned} \tag{19}$$

In Fig. 4, we show the ratio of $N_1(\beta)$ to $N_1(\pi/2)$ and the ratio of $N_2(\beta)$ to $N_2(\pi/2)$ for the initial condition $\epsilon_0 = 20$ GeV/fm³ and $R_x = 3$ fm, $R_y = 4$ fm. Where β is the azimuthal angle of ϕ meson

$$\cos \beta = k_x/|\mathbf{k}_T|, \quad (|\mathbf{k}_T| = \sqrt{k_x^2 + k_y^2}). \tag{20}$$

The ratio of $N_1(\beta)$ to $N_1(\pi/2)$ and the ratio of $N_2(\beta)$ to $N_2(\pi/2)$ can express the levels of the elliptical anisotropy of $N_1(\mathbf{k})$ and $N_2(\mathbf{k})$ in Eq. (19), respectively. The ratio of $N_1(\beta)$ to $N_1(\pi/2)$ is almost equal to the ratio of $N_2(\beta)$ to $N_2(\pi/2)$ in low transverse momentum region, so the mass-shift does not affect the v_2 in this region. However,

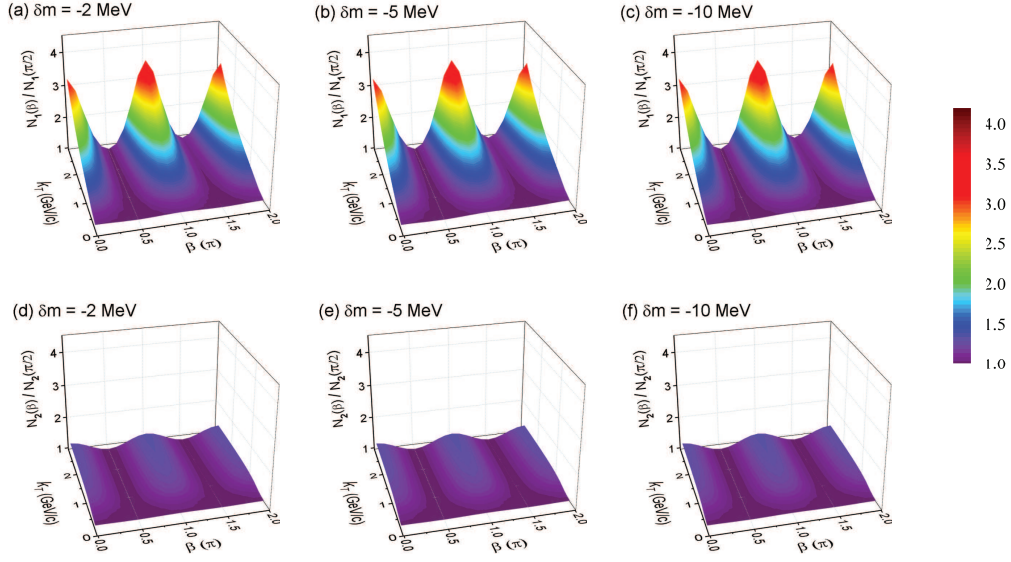


FIG. 4: (Color online) The ratio of $N_1(\beta)$ to $N_1(\pi/2)$ (top panel) and the ratio of $N_2(\beta)$ to $N_2(\pi/2)$ (bottom panel) in k_T - β plane for the initial condition $\epsilon_0 = 20 \text{ GeV/fm}^3$ and $R_x = 3 \text{ fm}$, $R_y = 4 \text{ fm}$.

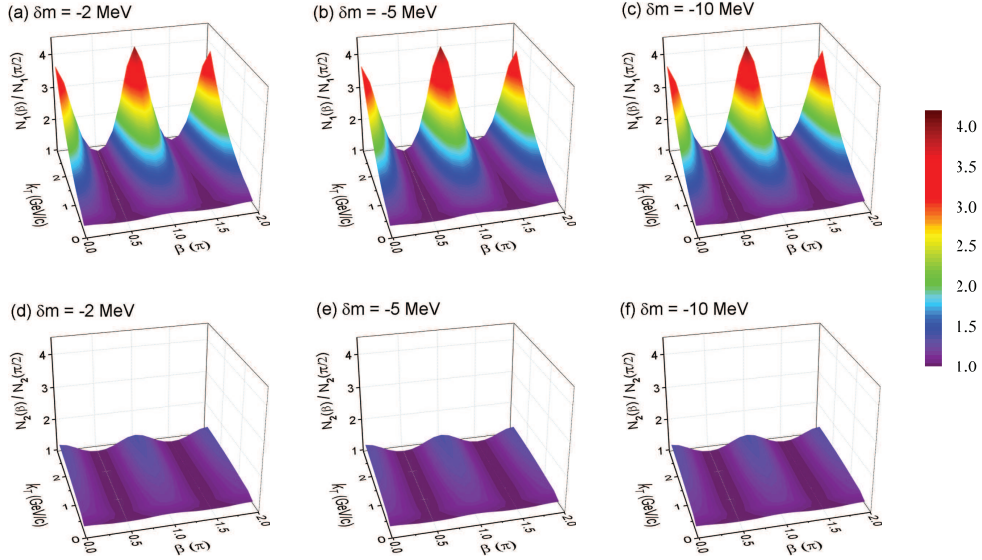


FIG. 5: (Color online) The ratio of $N_1(\beta)$ to $N_1(\pi/2)$ (top panel) and the ratio of $N_2(\beta)$ to $N_2(\pi/2)$ (bottom panel) in k_T - β plane for the initial condition $\epsilon_0 = 40 \text{ GeV/fm}^3$ and $R_x = 3 \text{ fm}$, $R_y = 4 \text{ fm}$.

the elliptical anisotropy of $N_1(\mathbf{k})$ is much greater than $N_2(\mathbf{k})$ in large transverse momentum region, so the v_2 is suppressed by mass-shift in large transverse momentum region. Although the elliptical anisotropy of $N_2(\mathbf{k})$ is almost the same for different δm , but the ratio of $\overline{F_2}$ to $\overline{n'_{k'}}$ for large δm is greater than for small δm , so the v_2 is more suppressed by a large mass-shift.

In Fig. 5, we show the ratio of $N_1(\beta)$ to $N_1(\pi/2)$ and the ratio of $N_2(\beta)$ to $N_2(\pi/2)$ for the initial condition $\epsilon_0 = 40 \text{ GeV/fm}^3$. The elliptical anisotropy of $N_1(\mathbf{k})$

for $\epsilon_0 = 40 \text{ GeV/fm}^3$ is a little greater than for $\epsilon_0 = 20 \text{ GeV/fm}^3$ in large transverse momentum region, and thus leads to a more greater v_2 of ϕ meson without mass-shift for $\epsilon_0 = 40 \text{ GeV/fm}^3$ (see Fig. 3). The elliptical anisotropy of $N_2(\mathbf{k})$ for $\epsilon_0 = 20 \text{ GeV/fm}^3$ is almost the same as for $\epsilon_0 = 40 \text{ GeV/fm}^3$, but the ratio of $\overline{F_2}$ to $\overline{n'_{k'}}$ for $\epsilon_0 = 40 \text{ GeV/fm}^3$ is smaller than for $\epsilon_0 = 20 \text{ GeV/fm}^3$. And thus the v_2 for $\epsilon_0 = 40 \text{ GeV/fm}^3$ is less suppressed than for $\epsilon_0 = 20 \text{ GeV/fm}^3$ for a fixed mass-

shift.

C. Parts of all ϕ meson have a mass-shift

When parts of all ϕ meson have a mass-shift, the single particle momentum distribution becomes

$$N_*^p(\mathbf{k}) = (1-p) \int \frac{g_i}{(2\pi)^3} d^4\sigma_\mu(r) k^\mu n_{\mathbf{k}'}^0 + p \int \frac{g_i}{(2\pi)^3} d^4\sigma_\mu(r) k^\mu [F_1 n_{\mathbf{k}'} + F_2], \quad (21)$$

where p is the probability of ϕ meson with mass-shift.

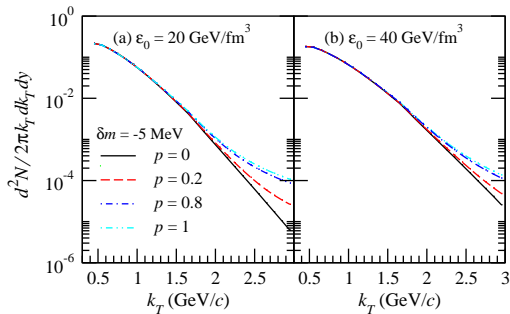


FIG. 6: (Color online) The normalized transverse momentum spectrum for parts of all ϕ meson have a mass-shift, where the initial conditions are the same as in Fig. 1.

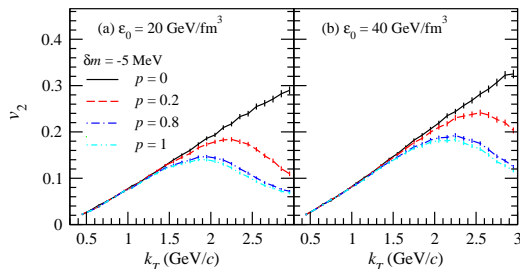


FIG. 7: (Color online) The v_2 for parts of all ϕ meson have a mass-shift, where the initial conditions are the same as in Fig. 3.

In Fig. 6 and 7, we show the normalized transverse momentum spectrum and v_2 for parts of all ϕ meson with mass-shift. The effect of mass-shift on the transverse momentum spectrum and v_2 decreases with the decreasing probability of ϕ meson with mass-shift.

The above results indicate that the different mass-shift leads to different transverse momentum spectrum and v_2 . The ranges of mass-shift of ϕ meson predicted by theory can be restricted by comparing the simulated transverse momentum spectrum and v_2 to the experimental data in high-energy heavy-ion collisions.

IV. SUMMARY

In this paper we studied the effect of in-medium mass-shift on the transverse-momentum spectrum and v_2 of ϕ meson. The mass-shift leads to an increase in the yield of ϕ meson in large transverse momentum region and thus reduce the slope of the transverse-momentum spectrum, and the elliptic flow v_2 of ϕ meson is suppressed by the mass-shift in large transverse momentum region. The effects of mass-shift on the transverse-momentum spectrum and v_2 increase with the increasing mass-shift. The effects also decrease with the increasing expanding velocity of the source. We further studied the effect of mass-shift on the transverse-momentum spectrum and v_2 for parts of all ϕ meson with mass-shift, and the effect of mass-shift on the transverse-momentum spectrum and v_2 decreases with the decreasing probability of ϕ meson with mass-shift. Our study may provide a way to restrict the ranges of mass-shift of ϕ meson by comparing the simulated transverse-momentum spectrum and v_2 to the experimental data in high-energy heavy-ion collisions.

Acknowledgments

This research was supported by the National Natural Science Foundation of China under Grant No. 11647166, 11747155, the Natural Science Foundation of Inner Mongolia under Grant No. 2017BS0104, Changzhou Science and Technology Bureau CJ20180054, and the Foundation of Jiangsu University of Technology under Grant No. KYY17028, KYY18048.

-
- [1] I. Arrsene *et al.* (BRAHMS Collaboration), Nucl. Phys. A **757**, 1 (2005).
 - [2] B.B. Back *et al.* (PHOBOS Collaboration), Nucl. Phys. A **757**, 28 (2005).
 - [3] J. Adams *et al.* (STAR Collaboration), Nucl. Phys. A **757**, 102 (2005).
 - [4] K. Adcox *et al.* (PHENIX Collaboration), Nucl. Phys. A **757**, 184 (2005).
 - [5] A. Shor, Phys. Rev. Lett. **54**, 1122 (1985).
 - [6] S.S. Adler *et al.* (PHENIX Collaboration), Phys. Rev. C **72**, 014903 (2005).
 - [7] B. Abelev *et al.* (STAR Collaboration), Phys. Rev. Lett. **99**, 112301 (2007).
 - [8] S. Afanasiev *et al.* (PHENIX Collaboration), Phys. Rev. Lett. **99**, 052301 (2007).
 - [9] B. Abelev *et al.* (STAR Collaboration), Phys. Lett. B **673**, 183 (2009).
 - [10] A. Adare *et al.* (PHENIX Collaboration), Phys. Rev. C **83**, 024909 (2011).
 - [11] A. Adare *et al.* (PHENIX Collaboration), Phys. Rev. C **92**, 044909 (2015).
 - [12] J.H. Chen, Y.G. Ma, and G.L. Ma *et al.*, Phys. Rev. C **74**, 064902 (2009).
 - [13] T. Hirano, U. Heinz, D. Kharzeev, R. Lacey, and Y. Nara,

- Phys. Rev. C **77**, 044909 (2008).
- [14] Md. Nasim, B. Mohanty, and N. Xu, Phys. Rev. C **87**, 014903 (2013).
- [15] L. Adamczyk *et al.* (STAR Collaboration), Phys. Rev. Lett. **116**, 062301 (2016).
- [16] B. Abelev *et al.* (ALICE Collaboration), JHEP **06**, 190 (2015).
- [17] T. Hatsuda and S.H. Lee, Phys. Rev. C **46** R34 (1992); T. Hatsuda, Nucl. Phys. A **544**, 27c (1992).
- [18] M. Asakawa and C.M. Ko, Nucl. Phys. A **572**, 732 (1994).
- [19] Chungsik Song, Phys. Lett. B **388**, 141 (1996).
- [20] W. Smith and K.L. Haglin, Phys. Rev. C **57**, 1449 (1998).
- [21] S. Pal, C.M. Ko, and Z. Lin, Nucl. Phys. A **707**, 525 (2002).
- [22] D. Cabrera and M.J. Vicente Vacas, Phys. Rev. C **67**, 045203 (2003).
- [23] E. Santini, G. Burau, Amand Fäßler, and C. Fuchs, Eur. Phys. J. A **28**, 187 (2006).
- [24] Volker Metag, Prog. Part. Nucl. Phys. **61**, 245 (2008).
- [25] J.D. Bjorken, Phys. Rev. D **27**, 140 (1983).
- [26] C. Shen, U. Heinz, P. Huovinen, and H.C. Song, Phys. Rev. C **82** 054904 (2010).
- [27] Y. Zhang, J. Yang, and W.N. Zhang, Phys. Rev. C **92** 024906 (2015).
- [28] M. Asakawa, T. Csörgő, and M. Gyulassy, Phys. Rev. Lett. **83** 4013 (1999).
- [29] S.S. Padula, G. Krein, T. Csörgő, Y. Hama, and P.K. Panda, Phys. Rev. C **73**, 044906 (2006).
- [30] Y. Zhang and W.N. Zhang, Eur. Phys. J. C **76** 419 (2016).
- [31] M. Asakawa and T. Csörgő, Heavy Ion Physics **4** 233 (1996); hep-ph/9612331.
- [32] F. Cooper and G. Frye, Phys. Rev. D **10**, 186 (1974).
- [33] P.F. Kolb and U. Heinz, arXiv:nucl-th/0305084.
- [34] P.F. Kolb, J. Sollfrank, and U. Heinz, Phys. Rev. C **62** 054909 (2000).
- [35] Y. Zhang, J. Yang, and W.N. Zhang, Chin. Phys. C **39** 034103 (2015).